

# Iron Emission Lines from Extended X-ray Jets in SS 433: Reheating of Atomic Nuclei

Simone Migliari,<sup>1\*</sup> Rob Fender,<sup>1\*</sup> Mariano Méndez,<sup>2</sup>

<sup>1</sup>Astronomical Institute ‘Anton Pannekoek’, University of Amsterdam, Kruislaan 403,  
1098 SJ Amsterdam, The Netherlands

<sup>2</sup>SRON, National Institute for Space Research, 3584 CA Utrecht, The Netherlands

\*To whom correspondence should be addressed; E-mail:  
migliari@astro.uva.nl (S.M.); rpf@astro.uva.nl (R.F.)

Powerful relativistic jets are among the most ubiquitous and energetic observational consequences of accretion around supermassive black holes in active galactic nuclei and neutron stars and stellar-mass black holes in x-ray binary (XRB) systems. But despite more than three decades of study, the structure and composition of these jets remain unknown. Here we present spatially resolved x-ray spectroscopy of arc second-scale x-ray jets from the XRB SS 433 analyzed with the Chandra advanced charge-coupled device imaging spectrometer. These observations reveal evidence for a hot continuum and Doppler-shifted iron emission lines from spatially resolved regions. Apparently, in situ reheating of the baryonic component of the jets takes place in a flow that moves with relativistic bulk velocity even more than 100 days after launch from the binary core.

The jets of XRB SS 433 are well established, quasi-persistent and the best example of regular precession of the jet axis (1–3). Extensive observing campaigns have placed constraints on the emission physics, geometry and scales associated with the baryonic component of the jets of SS 433. The generally accepted model for the thermal component of the jet is an adiabatic cooling model (4, 5). This model assumes that the emitting matter is moving along ballistic trajectories and expanding adiabatically in a conical outflow, and that the temperature and matter density are only a function of the distance from the core. The matter is ejected (the physical processes of ejection are still uncertain) with a temperature of  $> 10^8$  K (mean thermal energy per particle  $kT > 10$  keV) (4–6), comparable to that measured for the inner regions of accretion disks. Close to the binary core, at distances less than  $\sim 10^{11}$  cm, this jet plasma emits high-temperature continuum and Doppler-shifted lines in the soft x-ray band (6). The jet subsequently emits Doppler-shifted optical emission lines that are constrained to originate at distances of less than  $\sim 10^{15}$  cm because of a lack of measurable offsets between blue- and red-shifted beams. Neither line-emitting region has been spatially resolved from the core of SS 433. Furthermore, the temperature of the optical line-emitting region is limited to less than  $\sim 10^4$  K by the absence of higher excitation lines such as He II and C III/N III (7). In the adiabatic model the temperature decreases with the radial distance  $R$  from the core as temperature  $T \propto R^{-4/3}$ ; thus, at distances greater than  $\sim 10^{16}$  cm, the matter is expected to be at a temperature of  $< 100$  K, too cool to thermally emit x-ray and optical radiation. Besides this thermal radiation, there is nonthermal synchrotron radiation, which traces the distribution of relativistic electrons and the magnetic field in the jet, observed in the radio band at distances between  $10^{15}$  and  $10^{17}$  cm (2). Further out, the jet is not detected again until degree-scale (i.e., at distances of  $\sim 10^{19}$  to  $10^{20}$  cm from the binary core) termination shocks are observed, deforming the surrounding W50

nebula (Fig. 1, top), which is thought to be a supernova remnant associated with the formation of the neutron star or black hole in SS 433 (8, 9).

Marshall *et al.* (6) have recently analyzed the x-ray line emission from SS 433 with the Chandra high energy transmission grating spectrometer (HETGS). They refined the adiabatic cooling model, limiting the thermal x-ray emission region to within  $\sim 10^{11}$  cm of the jet base. They also discovered faint arc sec-scale x-ray emission on either side of the core, but they were not able to measure any emission lines and concluded that the jet gas would be too cool at such a distance to emit thermal x-rays.

We have analysed a 9.6-ks observation from 27 June 2000 with the Chandra advanced charge-coupled device (CCD) imaging spectrometer (ACIS)-S. The reduced image (Fig. 1) resolves arc sec-scale x-ray jets approximately symmetrically placed on either side of a weaker core and aligned with both the sub-arc sec radio jets and degree-scale structures in W50. Analysis of the image indicates that photon pile-up (10) in the core artificially reduced the measured count rate there, although according to the orbital ephemeris of Dolan *et al.* (11), our observation was close to x-ray eclipse, phase  $\sim 0.9$  (12), which may also have reduced the core flux. At a distance of 5 kpc, these x-ray jets correspond to physical scales of  $\geq 10^{17}$  cm and soft x-ray (2 to 10 keV) luminosities of  $3 \times 10^{33}$  to  $4 \times 10^{33}$  erg s $^{-1}$  each (about 3% of the average source total luminosity).

We were able to spatially isolate and take x-ray spectra of the two jets. The spectra of the two lobes between  $\sim 0.8$  and 10 keV (Fig. 2) can be fit by a bremsstrahlung continuum with a temperature of  $\sim 5$  keV and Gaussian emission lines at  $\sim 7.3$  keV for the approaching (east) jet and at  $\sim 6.4$  keV for the receding (west) jet (Table 1). In both spectra there is an indication of additional emission, possibly also lines, at higher energies, but this is near to the limit of the Chandra sensitivity, and given our relatively low count rates, we did not attempt to fit this component. A hydrogen column density

of  $\sim 10^{22} \text{ cm}^{-2}$  was found for both lobes, consistent with the column density found by Marshall *et al.* (6) for the core of SS 433. A power law with a photon index of  $2.1 \pm 0.2$  fits the continuum equally well, and on the basis of our current data, we cannot distinguish between a power law and bremsstrahlung for the continuum emission.

The significantly different line centroid energies measured for the east and west jets suggest that they may originate in the moving jet material. To test this hypothesis, we developed a model that sums the emission from ten equally spaced phase bins (13) around the precession cycle, calculating for each bin the Doppler shift  $\delta$  (14) and Doppler boosting of the line peak intensity  $\delta^2$  (assuming that the jets are intrinsically symmetric about the precession axis and east to west). A simulation based on this model for a 10-ks observation, assuming a rest energy for the line of 7.06 keV, corresponding to Fe XXV  $k\beta$  and using the same normalizations for the Gaussians as found in our observation, corresponds well to our data (Fig. 3 and Table 1).

The line energies and widths we obtain in our simulation are a good match to those measured in our observation (Fig. 2 and 3). Thus, we infer that the jet is emitting around the precession cone at a large distance from the core. Our model predicts twin-peaked lines, due to the distribution of Doppler shifts as a function of time, with a stronger blue peak (due to Doppler boosting); however, this twin-peak is not seen in the 10-ks simulation, which have a relatively low signal-to-noise ratio. However, if our model is correct, then additional observations should reveal this structure. Although we cannot use our model to conclusively establish that the Doppler-shifted line is Fe XXV  $k\beta$ , we do need a transition of hot, highly ionized Fe in order to achieve a high enough energy for the line in the east jet. We cannot exclude an origin for the  $\sim 6.4$  keV line in the west jet from neutral Fe; however, we cannot envisage a plausible geometry whereby we are observing neutral Fe at 6.4 keV in the west jet and the same line extremely blue-shifted

in the east jet. A further prediction of this model is that the east jet should be stronger than the west jet as a result of the overall larger Doppler boosting. The ratio of 2 to 10 keV fluxes (line and continuum) from the east to west jets is  $\sim 1.3$ , approximately what would be expected for the model considered here. Although we cannot explicitly show that the source of the continuum emission arises in the moving jet gas, the measured bremsstrahlung temperature is consistent with an origin in the same plasma as the high-excitation Fe lines. We therefore conclude that we observed lines, and probably also continuum, from a hot ( $> 10^7\text{K}$ ) plasma which is moving with a similarly high velocity to that measured for the “inner” jets (6),  $\sim 0.26c$  (where  $c \sim 3 \times 10^{10} \text{ cm s}^{-1}$  is the speed of light), on scales of  $10^{17} \text{ cm}$  from the binary core.

This is contrary to the adiabatic cooling model (4-6) which at that distance predicts that the baryonic component will have cooled to the ambient interstellar medium temperature; therefore, the jet has to re-heat itself. The most plausible energy source is the kinetic energy ( $\sim 10^{38} \text{ ergs/s}$ ) associated with the bulk motion of the jet (6). Because we observed optical emission lines coming from matter with temperatures of  $< 10^4 \text{ K}$  at a distance of  $\sim 10^{15} \text{ cm}$ , this re-heating must occur between  $\sim 10^{15}$  and  $10^{17} \text{ cm}$  from the core.

Alternatives to this scenario can be considered. A power law fits the continuum well, and by analogy with the extended x-ray jets seen in active galactic nuclei (AGN) (15), we cannot exclude an inverse-Compton or synchrotron origin for the continuum component. However, because both of these emission mechanisms require a population of hot electrons, they also imply reheating at those large distances from the central source. Regardless of which form of reheating is associated with the continuum spectrum, the emission lines require a baryonic component. Reflection of the core emission does not seem possible because the line flux we observed at  $10^{17} \text{ cm}$  is only a factor of  $\sim 10$  less than that

observed to originate at  $10^{12}$  cm (6), and yet our images indicate it does not subtend a significantly larger solid angle than the jets on smaller scales. Furthermore, the line to continuum flux ratio we observed is an order of magnitude greater than in the core [ $F_{\text{line}}/F_{\text{continuum}}$  is  $\sim 1$  for our east jet, but is  $\sim 0.1$  for the 7.3-keV line in Chandra HETGS observations (6)]. The lines from these extended jets are still an order of magnitude weaker than the moving core x-ray lines (5, 6), and would not be expected to show measurable changes in their Doppler shifts (unless, e.g., a major outburst from SS 433 resulted in enhanced emission at some particular precession phase). Nevertheless, they should be present as weak features in spectra that do not spatially resolve the core and jets.

Reheating (in situ acceleration) of a leptonic (electron and possibly also positron) component of jet plasma, presumably by conversion of the jet kinetic energy, is commonly invoked to explain synchrotron or inverse Compton energy emission on large scales in the jets of AGN (15-17). The reheating of the baryonic plasma that we observed in SS 433 requires a similar tapping of the bulk kinetic energy of the flow, by processes that are able to act on atomic nuclei. In the internal shock model for blazars (16), a slightly varying jet speed results in shocks downstream in the jet flow. In the context of this model, random discrepancies of about 15% in the velocity of the jets from SS 433, inferred from long-term optical monitoring (3), could produce shocks a few hundred days downstream (for a precession period of 162 days and a mean jet velocity of  $0.26c$ ), comparable to what we observed (18).

To conclude, these observations spatially resolve a line-emitting region in a relativistic jet. They reveal that the hot x-ray emitting region is still moving relativistically on physical scales that are orders of magnitude larger than previously inferred, with no evidence for substantial deceleration, supporting models for extended x-ray jets in AGN that require bulk relativistic motion on large physical scales (15). Furthermore, this observation

demonstrates that particle reacceleration in a relativistic jet, previously inferred only to act on the leptonic component, can act also on atomic nuclei. Comparison of this highly super-Eddington, mass-loaded jet with those of other x-ray binary systems and AGN can provide unique insights into the matter and energy content of relativistic jets and hence the coupling of accretion and outflow in conditions of extreme gravity, pressure, and energy density.

### References and Notes

1. G. O. Abell and B. Margon, *Nature* **279**, 701 (1979).
2. R. M. Hjellming and K. J. Johnston, *Nature* **290**, 100 (1981).
3. S. S. Eikenberry, *et al.*, *Astrophys. J.* **561**, 1027 (2001).
4. W. Brinkmann, N. Kawai, M. Matsuoka, H. H. Fink, *Astron. Astrophys.* **241**, 112 (1991).
5. T. Kotani, N. Kawai, M. Matsuoka, W. Brinkmann, *Publ. Astron. Soc. Pac.* **48**, 619 (1996).
6. H. L. Marshall, C. R. Canizares, N. S. Schulz, *Astrophys. J.* **564**, 941 (2002).
7. J. Shaham, *Vistas Astron.* **25**, 217 (1981).
8. W. Brinkmann, B. Aschenbach, N. Kawai, *Astron. Astrophys.* **312**, 306 (1996).
9. G. M. Dubner, M. Holdaway, W. M. Goss, I. F. Mirabel, *Astron. J.* **116**, 1842 (1998).
10. Pile-up is an effect by which two or more photons that hit the same pixel on the CCD in one integration are counted as a single photon. If

the summed energy is greater than the ACIS threshold ( $\sim 15$  keV), the detection is rejected, and no counts are recorded.

11. J. F. Dolan, *et al.*, *Astrophys. J.* **327**, 648 (1997).
12. The orbital phase  $0 \leq \phi \leq 1$  indicates the fraction of one entire orbit completed. Eclipse of the x-ray source (i.e., superior conjunction of the neutron star or black hole) corresponds to  $\phi = 0$ . The orbital period is 13.08 days.
13. The precession phase  $0 \leq \psi \leq 1$  indicates the fraction of one entire jet precession cycle.  $\psi = 0$  is, by convention (2), one of the two instances when the beams of SS 433 are perpendicular to the line of sight. The precessional period is 162.4 days.
14. The Doppler factor  $\delta = [\gamma(1 - \beta \cos \theta)]^{-1}$  where the velocity  $v = \beta c$ ,  $c$  is the speed of light,  $\gamma = (1 - \beta^2)^{-1/2}$  is the Lorentz factor, and  $\theta$  is the angle to the line of sight.
15. D. E. Harris and H. Krawczynski, *Astrophys. J.* **565**, 244 (2002).
16. M. Spada, G. Ghisellini, D. Lazzati, A. Celotti, *Mon. Not. R. Astron. Soc.* **325**, 1559 (2001).
17. G. V. Bicknell and D. B. Melrose, *Astrophys. J.* **262**, 511 (1982).
18. The relationship  $\Delta t = P(1 - \delta)/2\delta$ , where  $P$  is the precession period and  $\delta$  is the fractional deviation from the mean velocity  $v_m$  of the ejected blobs, gives the time interval  $\Delta t$  over which a blob with velocity  $(1 + \delta)v_m$  reaches the blob launched with velocity  $(1 - \delta)v_m$  at the same precessional phase one cycle earlier. Using  $P = 162$  days and  $\delta = 0.15$  we obtain  $t \sim 450$  days.



19. Fig. 1 (top) is reproduced by permission of the American Astronomical Society (Fig. 1 in (9)).
20. We thank Dan Harris and Michiel van der Klis for comments on a draft of this manuscript, and Wolfgang Brinkmann and Mike Watson for earlier useful discussions. MM and RF are grateful to Max-Planck-Institut für Astrophysik for their hospitality during the initial analysis of these data.

Table 1: Comparison of observed line centroid energies  $E$  and widths  $\sigma$  with simulations based on symmetric jets integrated over an entire precession cycle and a rest wavelength of 7.06 keV (Fe XXV  $k\beta$ ).

	$E_{\text{East}}$ (keV)	$\sigma_{\text{East}}$ (keV)	$E_{\text{West}}$ (keV)	$\sigma_{\text{West}}$
Observed	$7.28^{+0.02}_{-0.23}$	$0.7 \pm 0.2$	$6.39^{+0.12}_{-0.15}$	$0.2^{+0.2}_{-0.1}$
Simulated	$7.40^{+0.1}_{-0.2}$	$0.6 \pm 0.1$	$6.40^{+0.1}_{-0.1}$	$0.2^{+0.1}_{-0.2}$

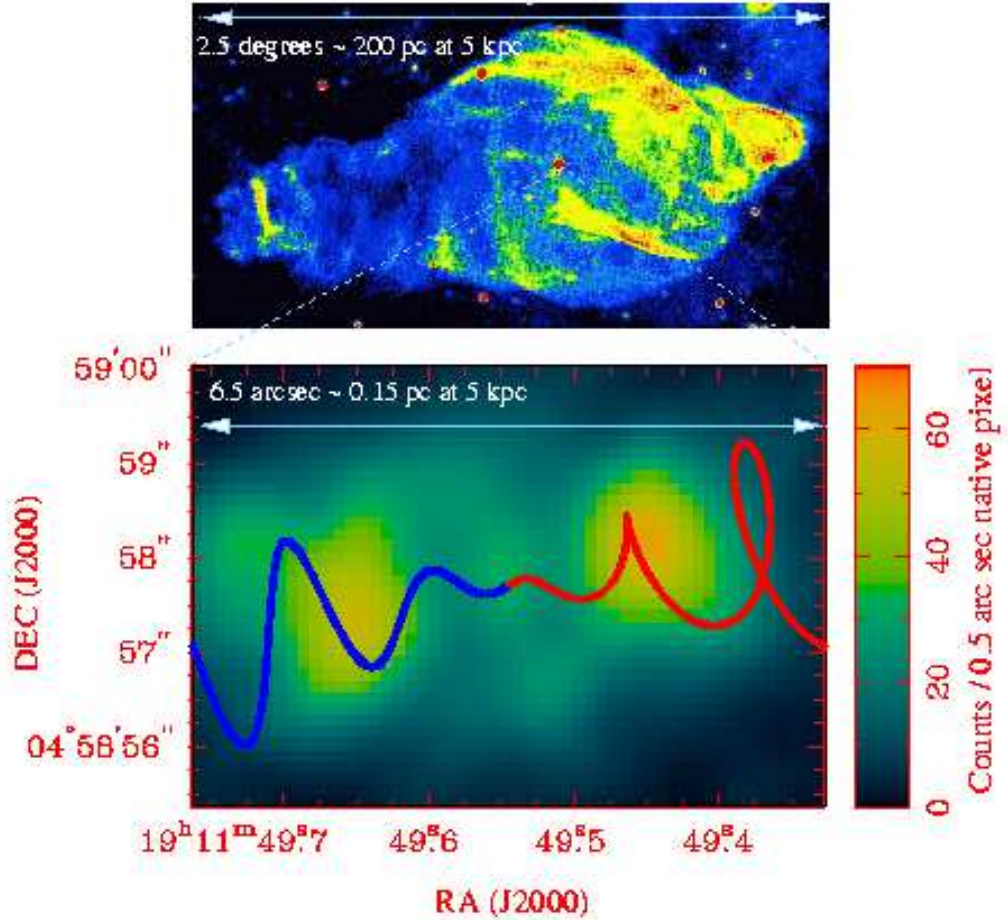


Figure 1: **(Bottom)** Image of SS 433 with Chandra ACIS-S, rebinned to one-quarter native pixel size and smoothed with a 0.5-arc sec Gaussian (comparable to the resolution of the telescope). The predicted projection on the sky of the jet precession cycle is indicated. The blue line refers to the jet that, for the most of the time, is approaching Earth (it is receding only  $\sim 16$  days over the 162-day precession cycle), and the red line refers to the (mostly) receding jet. The x-ray emission lies in the jet path and, while concentrated in two lobes, shows weaker emission extended beyond these to larger distances at the predicted position angles. **(Top)** Comparison with the surrounding W50 radio nebula (9) shows the correspondence in alignment of the structures, both of which reveal the signature of the jet precession (19). DEC, declination; RA, right ascension.

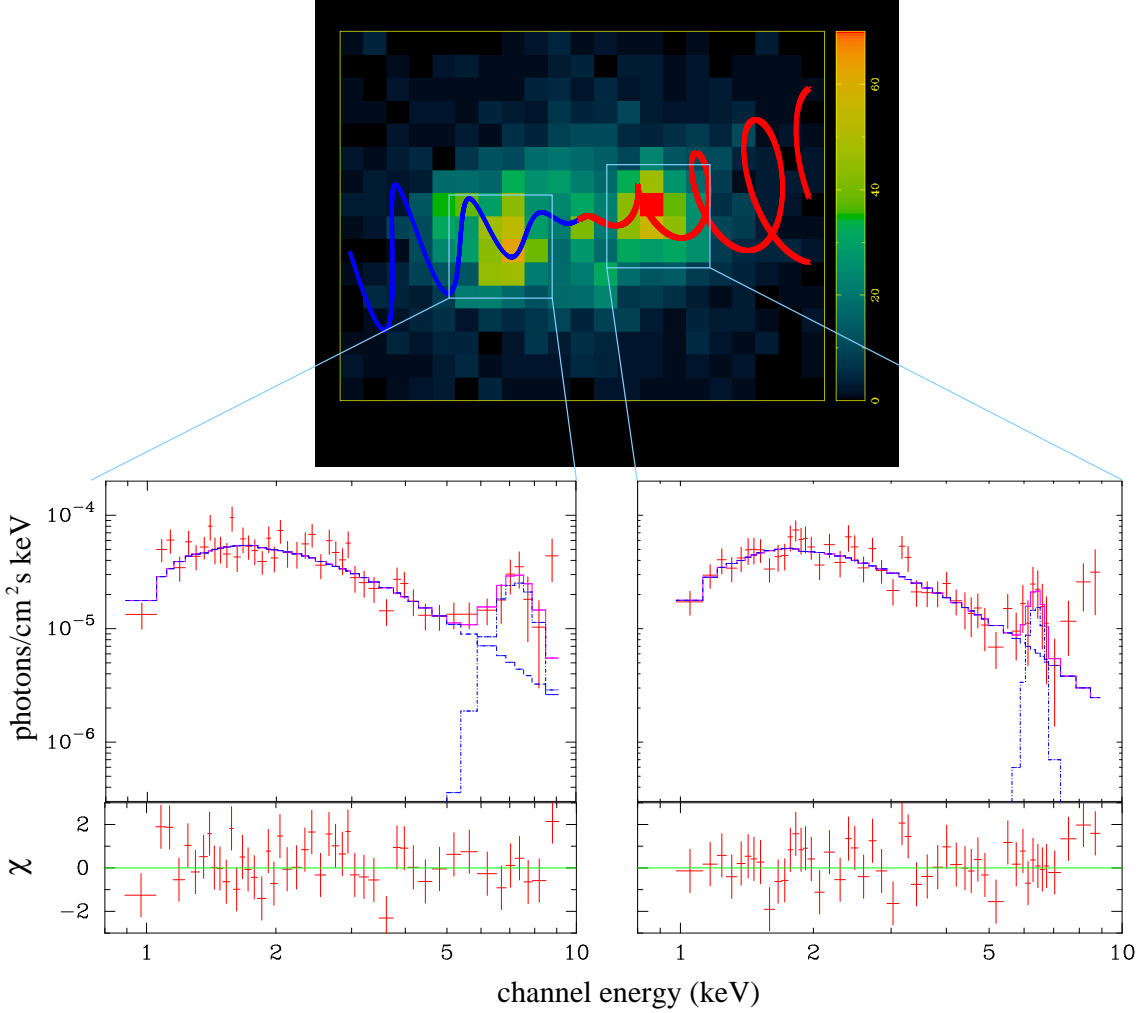


Figure 2: **(Top)** Raw (i.e., not regridded) Chandra ACIS-S image of SS 433 with the projected precession cycle of the jets superimposed on it, indicating the regions of the jet we isolated and analyzed. **(Bottom)** The two spectra of the lobes (crosses), east (left) and west (right), with the fitted model [absorbed bremsstrahlung (dashed line) and Gaussian emission line (dashed-dotted line)] and residuals ( $\chi$ ). The error bars represent the  $1\sigma$  confidence interval for each measurement; the residuals are plotted in units of  $\sigma$ .

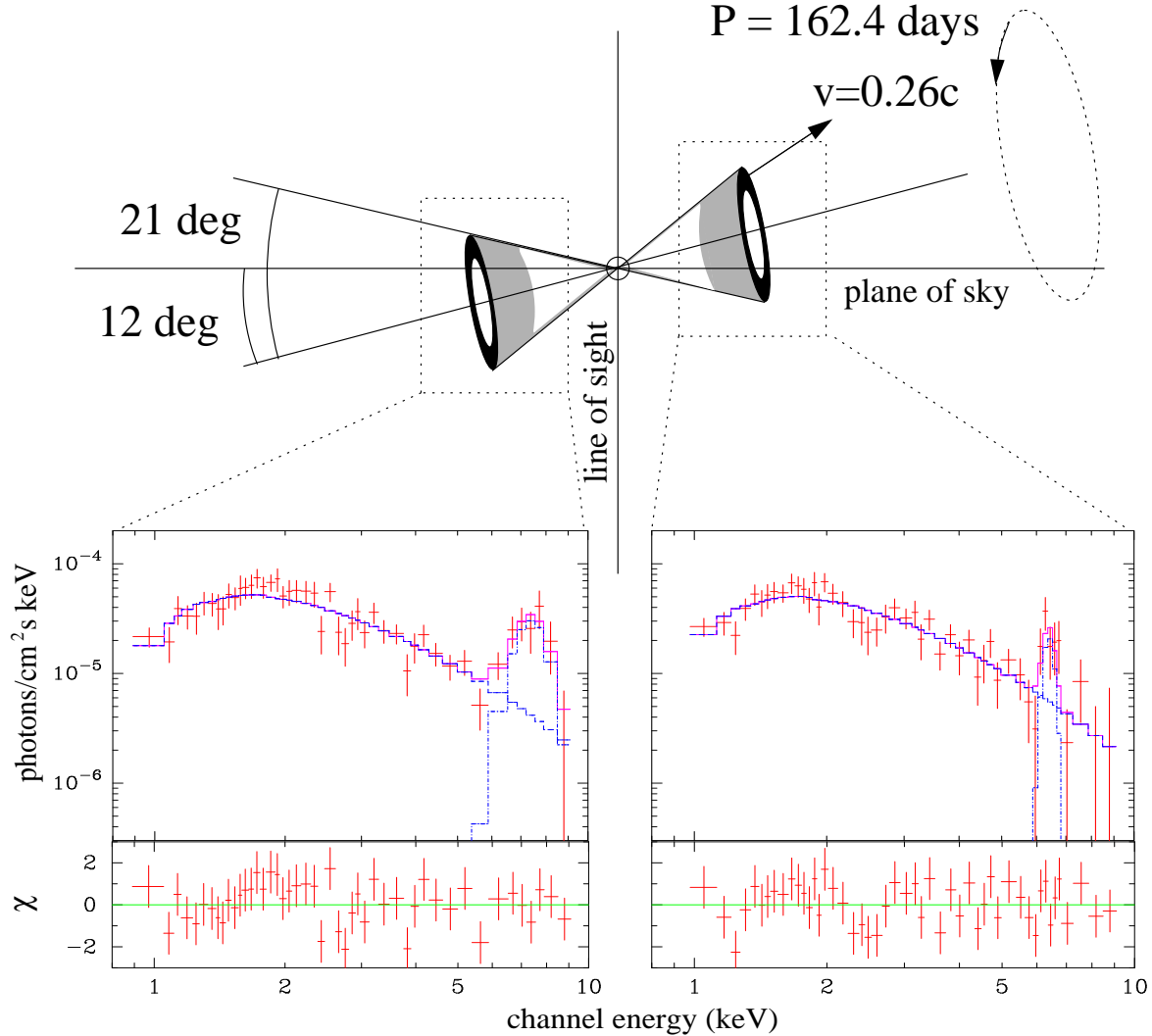


Figure 3: Simulated spectra (crosses), integrated over one entire precession cycle and fit for the same integration time, with the same binning and model [absorbed bremsstrahlung (dashed line) and Gaussian emission line (dashed-dotted line)] as for our observation in Fig. 2. Residuals ( $\chi$ ) of the fit are also plotted. The error bars represent the  $1\sigma$  confidence interval for each measurement; the residuals are plotted in units of  $\sigma$ . Parameters for the jet precession model (jet velocity  $v = 0.26c$ , opening angle  $\theta = 21^\circ$ , precession axis angle  $i = 78^\circ$ , period  $P = 162.4$  days) are from (3). For each of ten precession phases, the observed line energy  $E_{\text{obs}} = \delta E_{\text{rest}}$  and Doppler-boosted peak intensity  $I_{\text{obs}} = \delta^2 I_{\text{rest}}$  were calculated and summed to produce the resultant line profiles (the model can be visualized as simulating the integrated line emission of the shaded region in the schematic). The normalization of the summed lines was chosen to be the same as that in our observations, and the rest energy of the line was chosen to correspond to that of Fe XXV  $k\beta$  (i.e., 7.06 keV).